Archives of Toxicology (2022) 96:3201–3217
https://doi.org/10.1007/s00204-022-03362-7

INORGANIC COMPOUNDS

In vivo and in vitro toxicity of a stainless-steel aerosol generated during thermal spray coating

Vamsi Kodali[1,3] · Aliakbar Afshari[1] · Terence Meighan[1] · Walter McKinney[1] · Md Habibul Hasan Mazumder[3,4,5] · Nairrita Majumder[3,4] · Jared L. Cumpston[1] · Howard D. Leonard[1] · James B. Cumpston[1] · Sherri Friend[1] · Stephen S. Leonard[1,5] · Aaron Erdely[1,3,4] · Patti C. Zeidler-Erdely[1,3,4] · Salik Hussain[3,4] · Eun Gyung Lee[2] · James M. Antonini[1,3]

Received: 25 May 2022 / Accepted: 11 August 2022 / Published online: 19 August 2022

Abstract

Thermal spray coating is an industrial process in which molten metal is sprayed at high velocity onto a surface as a protective coating. An automated electric arc wire thermal spray coating aerosol generator and inhalation exposure system was developed to simulate an occupational exposure and, using this system, male Sprague–Dawley rats were exposed to stainless steel PMET720 aerosols at 25 mg/m^3 × 4 h/day × 9 day. Lung injury, inflammation, and cytokine alteration were determined. Resolution was assessed by evaluating these parameters at 1, 7, 14 and 28 d after exposure. The aerosols generated were also collected and characterized. Macrophages were exposed in vitro over a wide dose range (0–200 µg/ml) to determine cytotoxicity and to screen for known mechanisms of toxicity. Welding fumes were used as comparative particulate controls. In vivo lung damage, inflammation and alteration in cytokines were observed 1 day post exposure and this response resolved by day 7. Alveolar macrophages retained the particulates even after 28 day post-exposure. In line with the pulmonary toxicity findings, in vitro cytotoxicity and membrane damage in macrophages were observed only at the higher doses. Electron paramagnetic resonance showed in an acellular environment the particulate generated free radicals and a dose-dependent increase in intracellular oxidative stress and NF-kB/AP-1 activity was observed. PMET720 particles were internalized via clathrin and caveolar mediated endocytosis as well as actin-dependent pinocytosis/phagocytosis. The results suggest that compared to stainless steel welding fumes, the PMET 720 aerosols were not as overtly toxic, and the animals recovered from the acute pulmonary injury by 7 days.

Keywords Thermal spray coating · Metals · Particulates · Lung toxicity · Inhalation system

✉ Vamsi Kodali
ywu0@cdc.gov

[1] Centers for Disease Control and Prevention, National Institute for Occupational Safety and Health, Health Effects Laboratory Division, 1000 Frederick Lane (Mailstop 2015), Morgantown, WV 26508, USA

[2] Respiratory Health Division, National Institute for Occupational Safety and Health, Morgantown, WV 26505, USA

[3] Department of Physiology and Pharmacology, School of Medicine, West Virginia University, Morgantown, WV 26506, USA

[4] Center for Inhalation Toxicology (iTOX), School of Medicine, West Virginia University, Morgantown, WV 26506, USA

[5] Department of Pharmaceutical Sciences, School of Pharmacy, West Virginia University, Morgantown, WV 26506, USA

Introduction

Thermal spray coating is a process that involves spraying a metal coating product that is melted by extremely high temperatures (up to 16,000 °C) and then deposited under pressure onto various surface substrates made of metal and alloys, ceramics, or plastics (ASM; Oerlikon). When heated, the molten metal spray coating particles impact the surface at very high speeds, causing them to flatten and spread out over the substrate upon impact. The heated particles transfer heat to the cooler substrate, shrink, and solidify, resulting in a tight bond to the surface to be coated. Thermal spray coating processes are economical, simple to use, and beneficial to applications across nearly all industrial sectors including biomedical, automobile, aeronautical and construction (ASM; Gérard 2006; Hardwicke and Lau 2013; Herman et al. 2000; Malek et al. 2013). Uses of thermal spray coating include wear prevention, repair and restoration, decoration, insulation, conduction, sealing, corrosion resistance, and the manufacture of free-standing components.

A complex mixture of potentially toxic metals [e.g., chromium (Cr), nickel (Ni), zinc (Zn), iron (Fe), and aluminum (Al)] is generated during thermal spray coating processes that may pose an adverse health risk to the operator who often performs the process manually. The generated metal particulates are mostly in the fine and ultrafine size ranges (Antonini et al. 2021; Bemer et al. 2010). Workplace exposure levels of total and specific metals produced during thermal spray coating have been reported to be quite high (Bemer et al. 2010; Chadwick et al. 1997; Darut et al. 2021a; Huang et al. 2016; Petsas et al. 2007). However, information about the potential health effects associated with exposure to thermal spray coating aerosols is limited, and little is known about the physical and chemical properties of the aerosols generated during thermal spray coating (Antonini et al. 2021).

Occupational exposure to thermal spray coating aerosols is a potential emerging hazard, as the global market for thermal spray applications is predicted to be approximately 14.1 billion dollars by 2028 (ASM; GrandViewResearch). Nearly 138,000 workers were employed in coating and spraying machine operations in May 2020 (BLS). It is expected that these numbers will grow as the demand for thermal spray coating increases. Because thermal spray coating is an emerging industry and little is known about the associated health effects, studies are needed to characterize the aerosols generated as well as assess their potential toxicity in a controlled laboratory setting.

National Institute for Occupational Safety and Health (NIOSH) investigators have recently developed a novel and automated thermal spray coating aerosol generator and animal exposure system (Afshari et al. 2022). It was the goal of the current study to assess the pulmonary toxicity potential of the aerosols generated during flame spray thermal spray coating using a common consumable stainless-steel wire (PMET720). The PMET720 stainless steel wire is widely used for machine elements repair, dimensional restoration and wear resistant applications. Male Sprague–Dawley rats were exposed to a target animal chamber concentration of 25 mg/m^3 of the stainless-steel thermal spray coating aerosol for 4 h/day × 9 day. Lung inflammation, alteration in lung cytokine/chemokine response, injury and resolution with time, were assessed by evaluating lung parameters 1, 7, 14, and 28 d after the final exposure. Material characterization, acellular and in vitro toxicity were evaluated on two sets of PMET720 stainless steel samples, collected at settings of (1) 200 A, 60 psi, 30 V or (2) 200 A, 50 psi, 30 V. This allowed assessment about whether the process parameters affected the physicochemical characteristics and cellular toxicity of the thermal spray coating particles. The mechanism of internalization in macrophages was determined by using pharmaceutical inhibitors for clathrin-dependent endocytosis, caveolae-dependent endocytosis, and actin-dependent pinocytosis/phagocytosis. In addition to determining a dose–response relationship for in vitro toxicity to the PMET720 thermal spray coating particles in macrophages, cells were also screened for known cellular and molecular mechanisms of toxicity induced by well-characterized stainless steel welding fumes that were used as particle controls to estimate relative potency of the novel PMET720 thermal spray coating particles.

Materials and methods

Animals

Male Sprague–Dawley rats, from Hilltop Lab Animals (Scottdale, PA), were used. They weighed 250—300 upon arrival grams and were free of viral pathogens, parasites, mycoplasmas, *Helicobacter*, and CAR bacillus. The rats were acclimated for up to one week after arrival and were provided HEPA-filtered air, irradiated Teklad 2918 diet, and tap water ad libitum. All animal procedures used were reviewed and approved by the Centers for Disease Control and Prevention (CDC), Morgantown-NIOSH Animal Care and Use Committee (ACUC). The animal facilities are specific pathogen-free and environmentally controlled. The program and the facility are accredited by the AAALAC International (Frederick, MD).

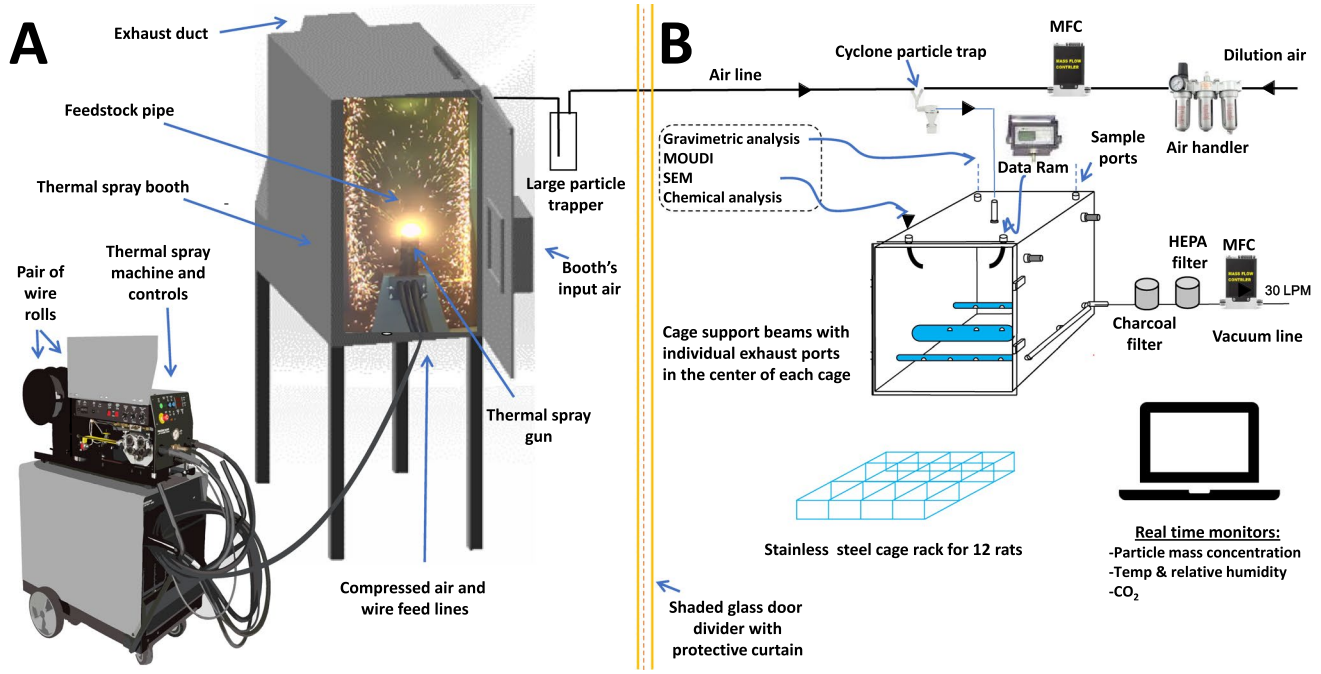

Fig. 1 Schematic diagram of the electric arc wire-thermal spray coating aerosol generator and exposure system (modified from Antonini et al. 2021; Afshari et al. 2022). Electric arc wire-thermal spray coating was performed in one room (**A**), and the aerosols transferred to an animal exposure chamber in a separate room (**B**) divided by shaded glass door divider with a protective curtain. Abbreviations: Data Ram = real-time aerosol monitor; MOUDI = Micro Orifice Uniform Deposit Impactor; SEM = scanning electron microscopy; Temp = temperature; LPM = liters per minute; MFC = mass flow controller

Thermal spray coating aerosol generation and exposure

A computer-controlled thermal spray coating generator and inhalation exposure system was constructed to perform animal studies to mimic workplace exposures in a laboratory [see diagram in Fig. 1; (Afshari et al. 2022)]. Rats were exposed by inhalation to aerosols (target concentration: 25 mg/m^3 × 4 h/day × 9 day) generated from electric arc wire thermal spray coating using a stainless-steel consumable wire (PMET720; Polymet Corporation, West Chester, OH) at settings of 200 A, 60 psi, and 30 V. Control animals were exposed to filtered air in a separate, identical exposure chamber.

The stainless-steel thermal spray coating aerosol was generated in a closed spray booth and transported to an animal exposure chamber where it was collected and characterized. At different post-exposure time points (1, 7, 14, and 28 d), the animals were humanely euthanized, and different makers of lung toxicity were measured. For the mechanistic in vitro studies, two sets of PMET720 stainless steel samples were collected onto filters at settings of (1) 200 A, 60 psi, 30 V or (2) 200 A, 50 psi, 30 V to assess whether the process parameters affect the physicochemical characteristics and cellular toxicity of the particles. In most assays, the responses were compared to different, well-characterized stainless steel welding particles that served as sample controls.

The thermal spray coating exposure system was divided into two separated areas (Fig. 1): (A) an enclosed room where the spray coating occurred that contained a compressed air tank, thermal spray machine with wire holder and feeder unit (AT-400 Wire Arc Spray System; Thermach, Inc., Medina, WI), the rotary and reciprocating system that holds and rotates the stainless-steel pipe to be spray coated in an up and down manner, and a spray coating booth that housed the torch gun and rotary sample holder system; (B) the animal exposure chamber with different particle characterization and chamber condition devices and air flow controllers. The room that contained the thermal spray coating booth was separated from the investigators by a set of protective curtains and glass door dividers to prevent exposure to the generated fumes and particles should the booth leak outward.

Within the spray booth, two consumable PMET720 stainless steel metal wires were fed independently into the spray gun. The wires were then charged, and an arc was generated between them. The heat from the arc melted the incoming wires, and the molten metal particles were suspended in a jet of air from the gun. The suspended molten metal particles were deposited onto the metal pipe substrate with the help of compressed air. A rotary motor rotated the feedstock pipe in

circular and up-and-down directions to allow for continuous, sequential coating during the 4-h exposure time within the spray booth. The spray gun was controlled by a computer program and was fired in 1 s intervals approximately 25 times total during the exposure period to produce a target concentration of 25 mg/m^3 in the exposure chamber.

The aerosols generated during the thermal spray coating process were delivered to an adjacent exposure chamber using a slight negative pressure. After leaving the booth the aerosol passed through a large particle trap then mixed with an automatically adjusted amount of diluted air. After the aerosol and dilution air mixed, it passed through a home-made large particle trap and mixed with diluted air before passing through a cyclone (URG-2000-30EP, URG Corp, Chapel Hill NC) to further remove large particles. The cut size of the cyclone was 6 μm at a flow of 31 L/min. The flow into the cyclone was maintained at 31 L/min, by using a mass flow controller connected to house vacuum on the exhaust side of the air-tight exposure chamber. Large particles were removed so that the animals would receive only the respirable portion of the particles.

The mass concentration in the chamber was monitored by a real-time aerosol monitor (DataRAM, MIE, Inc., Bedford, MA). The sensors and measurement devices were managed and controlled through a custom computer software programed written in LabVIEW (National Instruments Corporation, Austin, TX). To maintain a constant particle concentration in the exposure chamber, the software would make adjustments to the amount of dilution air that made up the 31 L/min entering the exposure chamber. For example, if the concentration needed to be higher than its current level it would automatically lower the dilution air thus pulling more aerosol from the spray booth. The feedback control algorithm used to control the dilution air was a Proportional-Integral-Derivative feedback (PID) controller. When the amount of dilution air dropped below 4 L/min the custom software would trigger first the feedstock pipe to rotate and move up and down in front of the thermal spray gun for few seconds before activating the thermal spray gun for a 1-s spray. This would increase dilution air flow to keep the exposure concentration from climbing too high, then the amount of dilution air needed would slowly drop until it was below 4 L/min and another spray would trigger. This process would repeat, typically 1 spray every 5 to 20 min, until the end of the desired exposure duration. Particle mass concentrations inside the animal chamber were determined by collecting airborne particles with two, 47-mm closed-face cassettes loaded with polytetrafluoroethylene filters followed by gravimetric analyses. These filter data were used every exposure run to calibrate the DataRAM. The target exposure chamber mass concentration could be selected in the software and was typically set to 25 to 30 mg/m^3 for all experiments.

Additional ports were located on the top of the chamber and used to measure chamber pressure and to collect additional particle samples for size distribution, chemical composition, and electron microscopy analyses. The air pressure and temperature and relative humidity inside the chamber were continually measured during the exposure period (Vaisala Temperature-Humidity Probe, model# HMP60; Woburn, MA). The levels of generated carbon dioxide (Vaisala CO_2 Probe, model# GMP252; Woburn, MA) were continuously monitored in the chamber during animal exposures and maintained below 5000 ppm.

Gas metal arc-stainless steel (GMA-SS) and manual metal arc stainless steel (MMA-SS) welding fume

For the in vitro toxicity and potency studies of the novel thermal spray coating particles, aerosol was collected from the exposure chamber and compared with the well-characterized welding fume particle samples from gas metal arc-stainless steel (GMA-SS) and a flux-covered manual metal arc stainless steel (MMA-SS) welding fumes. The GMA-SS and MMA-SS particle samples were generated and kindly gifted by Lincoln Electric Co. (Cleveland, OH). The fume samples were generated in an open fume chamber (volume of 1 m^3) by an experienced welder using stainless steel electrodes and collected on a 0.2 μm Nuclepore filters (Nuclepore Co.; Pleasanton, CA).

Thermal spray coating aerosol characterization

The generated thermal spray coating aerosols were collected in the breathing zone of the animals in the exposure chamber during the daily 4-h exposure. The animal chamber held 12 animals at a time. Multiple runs were performed to assess the responses at 1 and 7 d (n = 12 rats) and 14 and 28 d (n = 12 rats). Matching sets of controls were exposed to filtered air in a separate, identical chamber. The actual chamber concentration for the thermal spray coating aerosol was determined to be 24.9 mg/m^3 ± 2.1 standard error (SE) and 30.0 mg/m^3 ± 10.2 SE for the first and second exposures as measured by DataRAM and filter readings, respectively. Importantly, size distribution, particle morphology (FE-SEM), and metal composition profile (ICP-AES) did not change during the 4-h exposure period.

Aerodynamic particle size and morphology

The aerodynamic size distribution of the different thermal spray coating aerosols inside the exposure chamber was determined using a Micro-Orifice Uniform Deposit Impactor (MOUDI; MSP Model 110, MSP Corporation, Shoreview, MN). Particles were collected between the size ranges of 0.056–18 μm that were separated into 11 fractions. The

mass median aerodynamic diameter (MMAD) and geometric standard deviation (GSD) of the aerosol were determined from gravimetric measurements. To assess particle morphology, the different thermal spray coating particles were collected onto 0.2 μm pore size 47-mm Nuclepore polycarbonate filters (Whatman, Clinton, PA). The filters were mounted onto aluminum stubs using double-stick carbon tape and viewed using a Hitachi S4800 field emission scanning electron microscope (SEM; Hitachi High-Tech America, Boston, MA).

Hydrodynamic size and zeta potential

The hydrodynamic size or agglomerated particulate in aqueous suspensions was determined by Dynamic light scattering (DLS). Malvern Zetasizer Nano ZS90 (Worcestershire, UK) equipped with a 633 nm laser at a 90° scattering angle was used to estimate the agglomerate charge (zeta potential) and hydrodynamic size. Particles were prepared in stock solution of phosphate buffered saline (PBS) containing 0.6 mg/ml bovine serum albumin (BSA) at 5 mg/ml. All measurements were performed at a particle concentration of 25 μg/ml in water and cell culture media, while maintaining a constant temperature of 25 °C. Samples were equilibrated inside the instrument for two min, and five measurements, each consisting of at least five runs, were recorded.

Metal composition

Particle samples were collected inside the exposure chamber onto 5 μm pore size polyvinyl chloride membrane filters (SKC, Inc., PA) in 37-mm cassettes during thermal spray coating using a PMET720 consumable wire. The particles were digested, and the metals analyzed using inductively coupled plasma-atomic emission spectroscopy (ICP-AES) by the NIOSH contract laboratory, according to NIOSH method 7303 modified for hot block/HCl/HNO_3 digestion (NIOSH, 1994). Metal content of blank filters were also analyzed for control purposes.

Bronchoalveolar lavage

At 1, 7, 14, and 28 days after the final inhalation exposure, bronchoalveolar lavage (BAL) was performed to assess lung injury and inflammation. Animals were euthanized with an overdose of a pentobarbital-based euthanasia solution (> 100 mg/kg, IP; Fatal-Plus Solution, Vortech Pharmaceutical, Inc., Dearborn, MI) and then exsanguinated by severing the abdominal aorta. The right lung was first lavaged with a 1 ml/100 g body weight aliquot of calcium- and magnesium-free PBS, pH 7.4. The first fraction of recovered BAL fluid (BALF) was centrifuged at 500 × g for 10 min, and the resultant cell-free supernatant was saved for lung cell damage analysis. The right lung was further lavaged with 6-ml aliquots of PBS until 30 ml were collected. These samples also were centrifuged for 10 min at 500 × g and the cell-free BALF fraction was discarded. The cell pellets from all washes for each rat were combined, re-suspended in 1 ml of PBS buffer, counted, and differentiated.

Assessment of lung injury and inflammation

Lactate dehydrogenase (LDH) was measured in the first fraction of the cell-free supernatant recovered from the BALF as a general marker for lung toxicity. LDH activity was determined by measuring the oxidation of lactate to pyruvate coupled with the formation of NADH at 340 nm. Measurements were taken with a COBAS MIRA auto-analyzer (Roche Diagnostic Systems, Montclair, NJ). For the determination of lung inflammation, total cell numbers recovered by BAL were determined using a Coulter Multisizer II and AccuComp software (Coulter Electronics, Hialeah, FL). Cell suspensions (5×10^4 cells) were spun using a Cytospin 3 centrifuge (Shandon Life Sciences International, Cheshire, England) for 5 min at 800 rpm onto a slide. Cells (200/rat) were identified after labeling with Leukostat stain (Fisher Scientific, Pittsburgh, PA) as monocytes/alveolar macrophages (AM) and polymorphonuclear leukocytes (PMN).

Multiplex analysis of in vivo lung cytokines

Changes in the levels of cytokines and chemokine in the lung after exposure to PMET720 or air were determined by measuring the cytokine/chemokines in the first fraction of the bronchoalveolar lavage at day 1 and 7 after exposure using 27 Plex Rat Cytokine/Chemokine Array (Eve Technologies, Calgary, Canada; #RD27). The 27 cytokines measured, included vascular endothelial growth factor (VEGF), regulated upon activation, normal T cell expressed and presumably secreted (RANTES), growth-regulated oncogen/keratinocyte chemoattractant (GRO/KC), tumor necrosis factor-α (TNF-α), granulocyte colony-stimulating factor (G-CSF), granulocyte–macrophage colony-stimulating factor (GM-CSF), monocyte chemoattractant protein-1 (MCP-1), interferon γ-induced protein 10 kDa (IP-10), leptin, liposaccharide-induced CXC chemokine (LIX), interleukins IL-1α, IL-1β, IL-2, IL-4, IL-5, IL-6, IL-10, IL-12(p70), IL-13, IL-17A, IL-18, macrophage inflammatory protein 1-α (MIP-1α), macrophage inflammatory protein 2 (MIP-2), epidermal growth factor (EGF), fractalkine and interferon-γ (IFN)-γ. The standard curves for each cytokine/chemokine had a range of 0 to > 25,000 pg/ml. Regression analysis of the standard curves helped determine the concentration of the cytokine/chemokine in the BAL samples. The assay

sensitivity for these markers ranged from 0.1 to 33.3 pg/ml. Data are presented as a heatmap of fold change in protein expression from control group (air-exposed) at 1 and 7 d after last day of inhalation exposure. The protein concentrations in pg/ml from the 24 animals, control air group (n = 6, 2 × time points) and PMET720 (60 psi) thermal spray coating group ($n = 6$, 2 × time points) is provided in the supplemental table.

Electron paramagnetic resonance

To detect and measure short-lived free radical intermediates, electron paramagnetic resonance (EPR) spin-trapping was used. To assess whether the thermal spray coating suspensions were capable of producing hydroxyl radicals ($OH^{\cdot}$), they were exposed to H_2O_2 through a Fenton-like reaction. Final concentrations were 100 mM of the spin-trap DMPO (5,5'-dimethylpyrroline N-oxide, Sigma-Aldrich, St. Louis, MO), 5 mg/ml the PMET720 samples, the GMA-SS and MMA-SS welding fumes (particle controls) or potassium dichromate [2 mM; Cr (VI) positive control], and 1 mM H_2O_2 suspended in PBS and mixed in the order listed. All reagents were mixed in test tubes for 3 min at room temperature, filtered through a Titan3 nylon 0.45 mm filter to halt the reaction and remove any metal particles. The sample was then transferred to a quartz flat cell for EPR measurement in a Bruker EMX spectrometer (Bruker Instruments Inc., Billerica, MA). For each sample, the instrument was set to run 3 scans with a 41 s scan time, a receiver gain of 1.0×10^4, a 40 ms time constant, 1.0 G modulation amplitude, 63.4 mW power, 9.751 frequency, and 3515 G magnetic field center. Samples were run in independent experiments ($n = 3$). Sample data were attained and processed as previously described (Leonard et al. 2004, 2003; Stefaniak et al. 2009). Briefly, signal intensity (peak height) from the 1:2:2:1 spectrum (characteristic for. OH) was used to measure the relative proportion of the short-lived radicals trapped.

In vitro cell culture, particulate collection and dispersion

The RAW 264.7 monocyte/macrophage cell line was obtained from American Type Culture Collection (Manassas, VA; ATCC TIB-71). The cells were cultured in Dulbecco's Modified Eagle medium (DMEM, Invitrogen) supplemented with 10% fetal bovine serum (FBS, R & D Systems, Minneapolis, MN), 1% antimycotic and 1% penicillin–streptomycin (Invitrogen, Waltham, MA) Subcultures were prepared by scraping and a sub-cultivation ratio of 1:4 was maintained. Cell culture media was replaced every 2 to 3 days. Cells were tested for mycoplasma; no mycoplasma contamination was detected.

The PMET720 particulate samples used for the in vitro study were collected directly from the generation chamber by gravity. The turbulence in the generation chamber was minimized by controlling flow, thus allowing the formed particulates to settle by gravity for 24 h into a clean collection vessel placed on the bottom of the floor of the generation chamber. The collected particulate samples were gently brushed from the collection vessel and stored into sterile, glass scintillation vials.

Aqueous stock suspensions of the dry PMET720 and welding fume control samples were prepared in PBS without calcium and magnesium at 5 mg/ml concentration and contains 0.6 mg/ml bovine serum albumin (BSA, Sigma-Aldrich). The stock suspension was sonicated for 1 min at 70% amplitude using a cup horn sonicator (Sonics Vibra-Cell VCX-750 with Cup-type Sonicator; Newton, CT) and immersed in continuous flowing cold water. Samples were vortexed for 10 s intermittently after 30 s of sonication. The stock solution at 5 mg/ml was dispersed in cell culture media by diluting to the highest test concentration, and serial dilutions were performed to obtain other concentrations.

In vitro cytotoxicity

Cytotoxicity due to particle exposure was accessed in RAW 264.7 cells by measuring the cells' ability to reduce water soluble tetrazolium salt (WST-1) and in parallel by measuring lactate dehydrogenase (LDH) released as a marker for membrane damage. Cells (25,000) were exposed for 24 h in 96 well plates to 0, 0.78, 1.56, 3.12, 6.25, 12.5, 25, 50, 100 and 200 µg/ml of PMET720 particles generated at 50 and 60 psi, and their potency was compared with the GMA-SS and MMA-SS welding particle samples in 100 µl of cell culture media. After 24 h of exposure, the supernatant was transferred to a new plate, and cells were challenged with fresh media containing 10% volume/volume WST-1 cell proliferation reagent (Sigma-Aldrich, Cat #5,015,944,001). After 2 h of incubation, the WST-1 consumption was recorded by measuring the absorbance at 450 nm subtracted with absorbance at 660 nm to account for turbidity/background. Data were presented as % change from control cells with no particulate treatment. Total LDH was evaluated by lysing cells with 0.1% volume/volume Triton X-100 (Sigma-Aldrich) for 1 h. Equal volume of cell culture media and CytoTox-ONE™ Reagent (Promega, Madison, WI) was reacted at room temperature and change in fluorescence was measured at excitation 560 nm and emission 590 nm. All experiments were repeated three times, and each measurement had quadruplicate technical replicates. Half-maximal inhibitory concentration (IC50) and half-maximal effective concentration (EC50) were determined by regression analysis of the experimental dose–response relationships.

In vitro oxidative stress

Intracellular oxidative stress due to particle exposure was determined using CellROX® Green (Invitrogen, Waltham, MA). Cells (7.5×10^5) were seeded in a 6-well plate and, after 18 h, they were challenged with 2 ml fresh media containing 0, 6.25, 25, 50 and 100 µg/ml of PMET720 sample generated at 50 and 60 psi or the GMA-SS welding fume sample. After 24 h of exposure, the cells were detached, washed, and incubated with 5 µM CellROX for 20 min. The CellROX treated cells were further washed and fixed with a 10% formaldehyde solution in PBS. The change in oxidative stress was quantified by evaluating the change in mean fluorescence per cell using a BD LSR II flow cytometer (BD Biosciences, San Diego, CA). At least 10,000 cells were quantified per treatment group and this was repeated three times.

In vitro NF-κB/AP1 activity

Monocyte/macrophage reporter cell line, RAW-Blue™ Cells (Invivogen, San Diego, CA) were used to evaluate NF-κB and AP-1 induced due to particulate exposure. Cells were exposed to the PMET720 particle sample generated at 50 or 60 psi, and their potency was compared with the GMA-SS and MMA-SS particle control samples. Cells were challenged with these four particle samples at 0, 1.56, 3.125, 6.25 and 12.5 µg/ml for 16 h. These doses were chosen based on cytotoxicity. The RAW Blue cells secrete alkaline phosphatase (SEAP) due to NF-κB and AP-1 activation. The induced SEAP was detected using alkaline phosphatase detection medium (QUANTI-Blue™ Solution, Invivogen, San Diego, CA) by measuring absorbance at optical density (OD) at 655 nm using a Varioskan™ LUX multimode microplate reader (Invitrogen).

In vitro mechanism of uptake

The mechanism of uptake of the PMET720 (60 psi) and GMA-SS particle samples in RAW 264.7 cells was evaluated as previously described (dos Santos et al. 2011; Ibuki and Toyooka 2012; Plummer and Manchester 2013; Suzuki et al. 2007; Vranic et al. 2013; Zucker et al. 2010). Chlorpromazine (15 µM; Invitrogen), 3 µM filipin III (Cayman Chemical Company, Ann Arbor, MI) or 8 µM cytochalasin B (Sigma-Aldrich) were used for inhibiting clathrin-mediated endocytosis, caveolin-mediated endocytosis and actin-dependent pinocytosis/phagocytosis, respectively. Cells were preincubated for 30 min with fresh media containing the inhibitors or media alone and then co-challenged with 50 µg/ml of PMET720 (60 psi), or GMA-SS with and without the inhibitors for 3 h. The cells were lifted and washed, and uptake was quantified by determining the granularity by flow cytometry (BD Biosciences, San Diego, CA). At least 10,000 cells were quantified per treatment group and is an average of three runs. Data were normalized by subtracting background with no particle exposure and is presented as percentage change from particulate uptake by control cells with no inhibitor treatment.

Statistical analysis

Statistical analyses were performed using either JMP version 13 (SAS Institute, Cary, NC) or using Prism (Graphpad Software LLC, CA). IC50 and EC50 values were determined by four-parameter logistic regression analysis in Prism. All the treatments were compared for statistical significance using factorial analysis of variance (ANOVA), either one- or two-way depending on the experimental design. ANOVA was followed by multiple comparison post hoc test for pairwise comparison using Tukey's or Fisher's Least Significant Difference (LSD). Differences were considered statistically significant at $p \leq 0.05$ (95% confidence level).

Results

Particle characteristics

Field-emission scanning electron microscopy (FE-SEM) and the size distribution graphs of the thermal spray coating aerosols generated at 60 and 50 psi are shown in Fig. 2. FE-SEM showed agglomerated chains of ultrafine-sized primary particles for the two generated PMET720 thermal spray coating aerosols (Fig. 2A, B). The mass median aerodynamic diameter (MMAD) and geometric standard deviation (GSD) of the aerosolized particles in the exposure chamber was 0.28 µm with a GSD of 1.8 at 50 psi and 0.31 µm with a GSD of 2.11 at 60 psi (Fig. 2C). To examine the in vitro toxicity of the PMET720 thermal spray particulate, macrophages in a 2-D submerged model was utilized, a stock dispersion of samples was prepared in PBS containing 0.6 mg/ml BSA and further diluted to the required concentration in cell culture media. DLS showed the thermal spray particle samples had a wide size distribution as indicated by the large polydispersity index (PDI). There was no statistically significant change in mean cumulative diameter with increasing pressure of the thermal spray (Table 1). There was a small but statistically significant decrease in charge of the thermal spray particulate with increasing pressure. The welding fume particle samples had narrower size distributions compared to the thermal spray particles. In addition, MMA-SS had a lower cumulative hydrodynamic diameter and GMA-SS had a larger diameter when compared to the PMET720 particle samples.

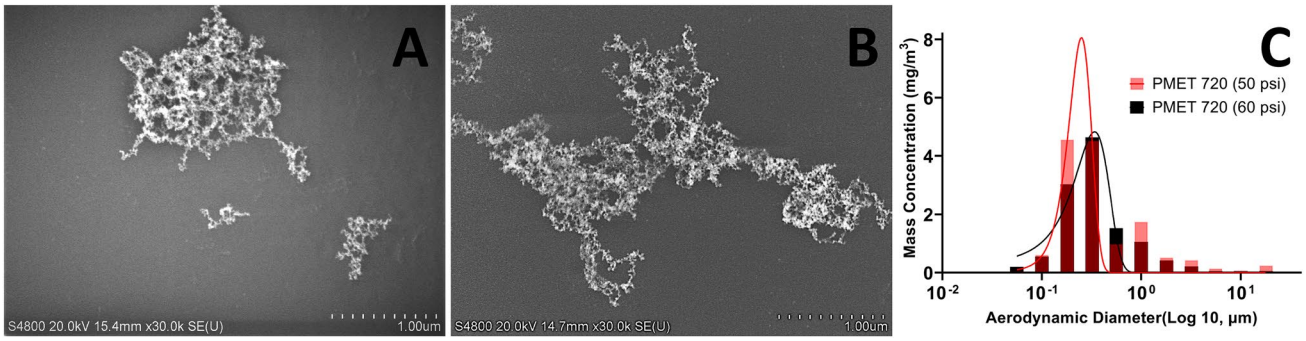

Fig. 2 **A**, **B** Representative FE-SEM micrographs of generated particles during electric arc wire-thermal spray coating (50 psi, 30 V, 200 A) and (60 psi, 30 V, 200 A) using a PMET720 stainless steel consumable wire, respectively, and (**C**) MOUDI particle size distribution graphs of each. Scale bar in A and B is 1 µm

Table 1 Particle sample characteristics

Particulate	Hydrodynamic Size[a,b]		Zeta Potential[a,b] (mV ± Stdev)	Mass Median Aerodynamic Diameter (MMAD, µm)	Geometric Standard Deviation (GSD)
	Cumulative Mean Diameter (nm ± Stdev)	Polydispersity Index (PDI)			
PMET720, 50 psi Thermal Spray Coating	472.3 ± 252.3	0.7 ± 0.2	– 13.5 ± 1.1	0.28	1.8
PMET720, 60 psi Thermal Spray Coating	431.3 ± 118.7	0.5 ± 0.2	– 15.5 ± 0.6	0.31	2.11
GMA-SS Welding Fume	868.3 ± 43.2	0.3 ± 0.1	– 14.8 ± 0.6	0.25	1.35
MMA-SS Welding Fume	338.5 ± 7.3	0.1 ± 0.1	– 11.3 ± 1.4	0.30	1.25

[a]Measurements were performed in PBS. [b]Measurements were performed at 25 °C at 25 µg/ml

Table 2 Metal composition of the collected particulate

	Fe	Cr	Mn	Zn	Ni	Cu	Ti	Al
PMET720 (50 psi)	81.7 ± 0.24	14.9 ± 0.19	2.61 ± 0.04	0.35 ± 0.08	0.26 ± 0.04	0.16 ± 0.002	ND	ND
PMET720 (60 psi)	82.2 ± 0.24	13.4 ± 0.14	2.37 ± 0.09	1.31 ± 0.13	0.397 ± 0.14	0.18 ± 0.013	ND	ND
GMA-SS Welding Fume	57.2 ± 1.2	20.3 ± 1.6	13.8 ± 0.47	ND	8.51 ± 0.40	ND	ND	0.085 ± 0.08
MMA-SS Welding Fume	42.0 ± 0.47	28.1 ± 0.26	16.2 ± 0.27	ND	2.84 ± 0.17	0.41 ± 0.0030	10.1 ± 0.30	ND

Relative weight % to all metals analyzed. ND: not detected or below detection limit

Metal composition analysis using ICP-AES showed that the major constituents in PMET720 thermal spray coating aerosols included Fe, Cr, Mn, Zn, Ni, and Cu (Table 2). The stainless-steel aerosols were predominantly composed of Fe and Cr. A change in pressure from 50 to 60 psi had little effect on the metal composition of the generated particles. Compared to GMA-SS and MMA-SS welding fumes, the thermal spray coating particles generated from PMET720 contained a greater amount of Fe but less Cr.

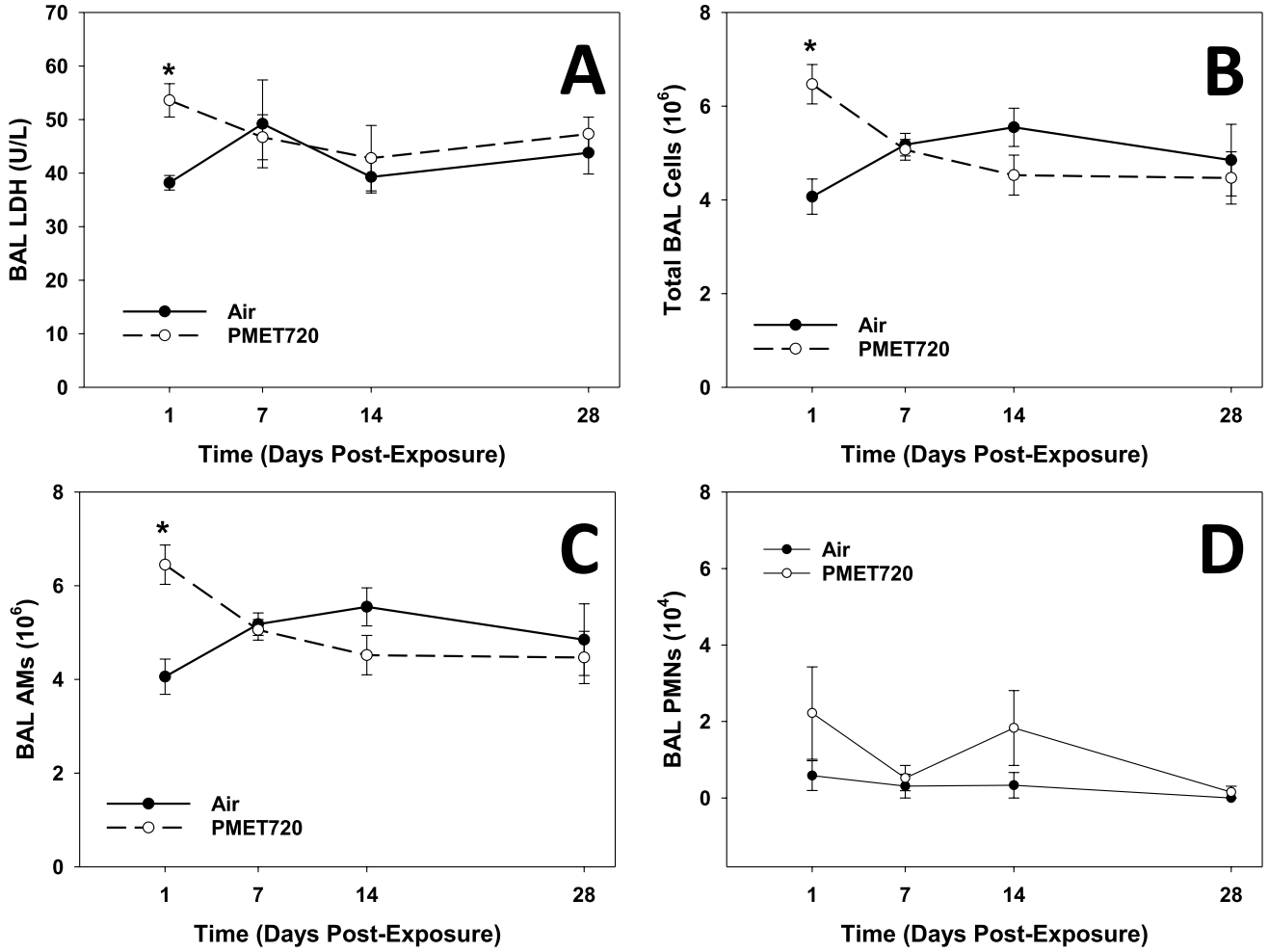

Fig. 3 Lung responses at 1, 7, 14, and 28 d after inhalation exposure to PMET720 stainless-steel thermal spray coating aerosol: **A** BAL LDH; **B** Total BAL cells; **C** BAL AMs; **D** BAL PMNs. Male Sprague–Dawley rats ($n = 5$–6/group) were exposed to 25 mg/m^3 of electric arc thermal spray aerosol using a PMET720 wire for 4 h/d × 9 d at 60 psi, 30 V, and 200 A. *Significantly different from air control exposure ($p < 0.05$)

In vivo pulmonary injury and resolution

The pulmonary injury induced by PMET720 (60 psi) thermal spray coating aerosols was assessed after inhalation exposure by measuring LDH in the first acellular fraction of the BALF at 1, 7, 14, and 28 d post-exposure to determine the resolution of the response. BALF LDH was significantly elevated at 1 d after the final exposure to the PMET720 stainless steel aerosol compared to the air control (Fig. 3A). By 7 day, the elevated LDH value had returned to control levels, and the groups were not significantly different up to 28 day after exposure.

In vivo pulmonary inflammation

In the determination of lung inflammation, the number of total BAL cells as well as BAL AMs and PMNs were counted at 1, 7, 14, and 28 d after the final exposure to the PMET720 thermal spray coating aerosol. At 1 d after the last exposure, total BAL cells and AMs were significantly increased in the PMET720 group compared to the control group (Fig. 3B, C). As was observed with the LDH response, the elevated total cell and AM numbers returned to air control levels by 7 d. No significant differences were observed for the number of BAL PMNs recovered when comparing the two treatment groups at any of the time points after exposure (Fig. 3D).

Figure 4A–E depicts representative images of recovered BAL cells after exposure to the PMET720 stainless steel thermal spray coating aerosols at 1, 7, 14, and 28 d. As indicated by the asterisks, numerous AMs had phagocytized particles (black pigmented material) inhaled by the lungs 1 d after exposure. As expected, the number of AMs that contained particles decreased with time after exposure,

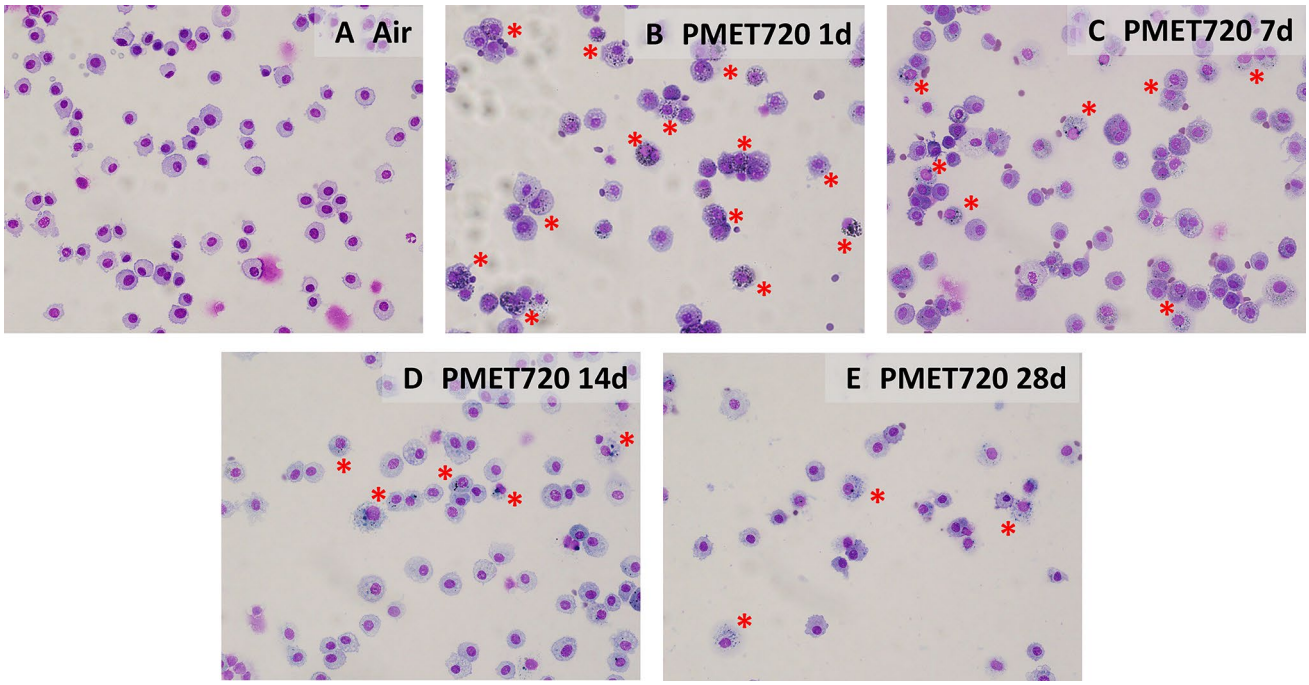

Fig. 4 Representative cytospin photomicrographs of recovered BAL cells after exposure to air (**A**; control) or 25 mg/m^3 of PMET720 stainless steel thermal spray coating aerosols at 1 (**B**), 7 (**C**), 14 (**D**), and 28 d (**E**). Red asterisks indicate particles (black pigmented material) within lung macrophages. Magnification is 40x

although numerous cells still contained engulfed particles at 28 d after exposure. In agreement with cellular differential data (Fig. 4 D), few PMNs were observed at any time point after exposure to the PMET720 (60 psi) aerosols.

Alteration in pulmonary cytokine/chemokine response

Alteration in lung cytokine/chemokines was assessed by screening 27 proteins in BAL fluid at 1 and 7 d after inhalation exposure to either air control or PMET720 (60 psi) thermal spray coating aerosols. Compared to air control, animals exposed to PMET720 thermal spray coating aerosols caused a significant change in seven BAL fluid proteins at 1 d after exposure (Fig. 5). The proteins that were altered included IL-18, MIP-1α, VEGF, LIX, fractalkine, IP-10, and EGF. The protein expression increased with all these proteins and was in the range of 1.5- to fourfold change from air control animals. The altered cytokine/chemokines play a vital role in tissue repair after a cytotoxic response and act as beacons for recruiting immune cells. At 7 d after PMET720 thermal spray coating exposure, the cytokines/chemokines reached homeostasis and only 2 proteins, MIP-1α and fractalkine, were significantly altered compared to air controls. The altered proteins at 1 d post-exposure were up-regulated while at 7 d they were down-regulated compared to air controls. The cytokine response was in line with the observed lung injury and cellular influx observed (Fig. 3A–D).

Comparative in vitro toxicity

The cytotoxicity potential of the PMET720 thermal spray coating particle samples generated at 60 and 50 psi was assessed using cell proliferation reagent WST-1 and in parallel, membrane damage evaluated by measuring LDH released. GMA-SS and MMA-SS, two well-characterized welding fumes, were used as controls to understand relative potency of the novel PMET720 thermal spray coating particles. The cells challenged with PMET720 (50) psi did not induce any cytotoxicity in the tested concentration range of (0–200 µg/ml). Only the highest dose tested (200 µg/ml) caused a significant change in cytotoxicity with the PMET720 (60) psi particulate. Both GMA-SS and MMA-SS welding fumes showed a dose-dependent increase in cytotoxicity and a significant change in cytotoxicity at and above 12.5 µg/ml (Fig. 6A). The IC50 for the PMET720 sample was > 200 µg/ml. The IC50 for GMA-SS and MMA-SS welding particles was 35 µg/ml ($R^2 = 0.9$, 95% CI 20.3–114.7 µg/ml) and 13 µg/ml ($R^2 = 0.99$, 95% CI 11.3–13.8 µg/ml), respectively.

Exposure of cells to PMET720 (50 psi) at 0–200 µg/ml did not induce significant membrane damage, whereas

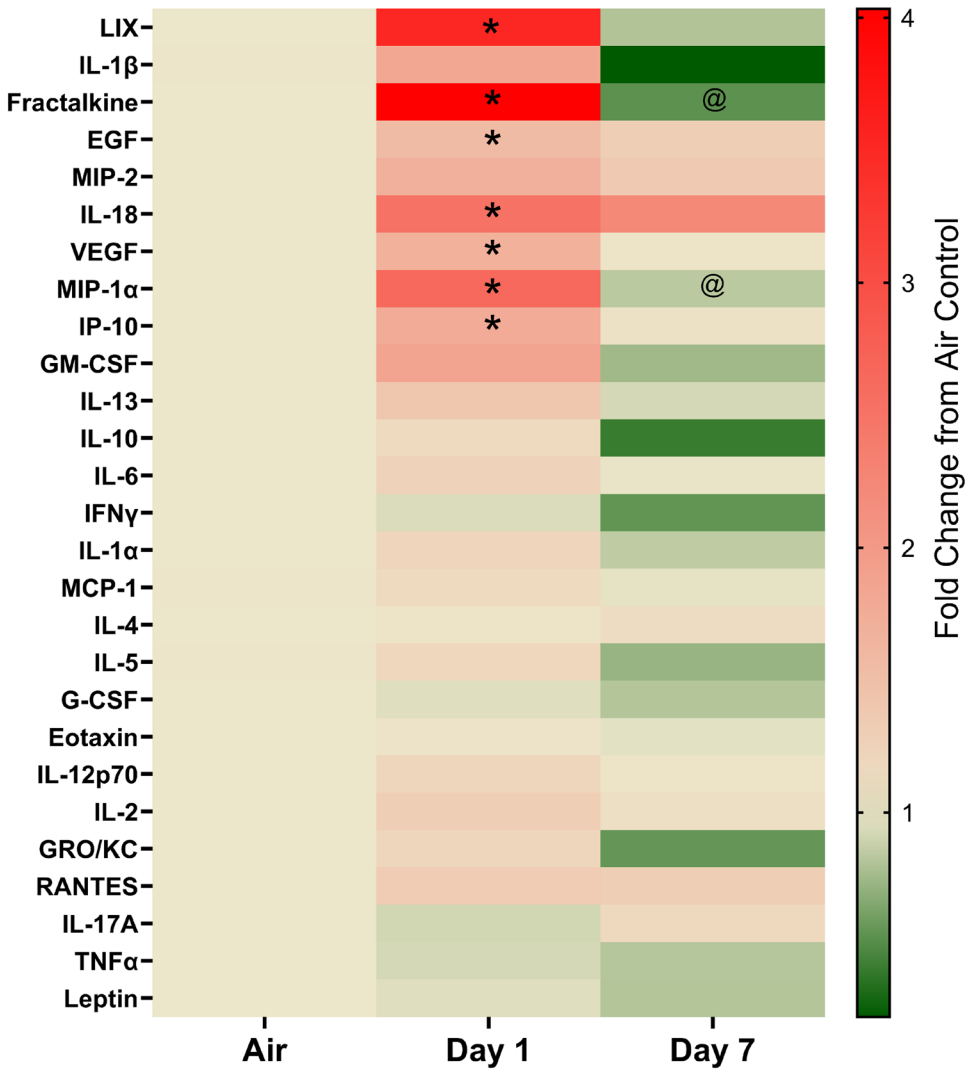

Fig. 5 Protein expression in BAL fluid after inhalation exposure to PMET720 (60 psi) stainless steel thermal spray coating aerosols accessed at 1 and 7 day after exposure. Data are represented as heat map of fold change from air control group. Two-way ANOVA was performed. *Denotes significance ($p < 0.05$) compared 1-day Air group; @ denotes significance from 7-day Air group

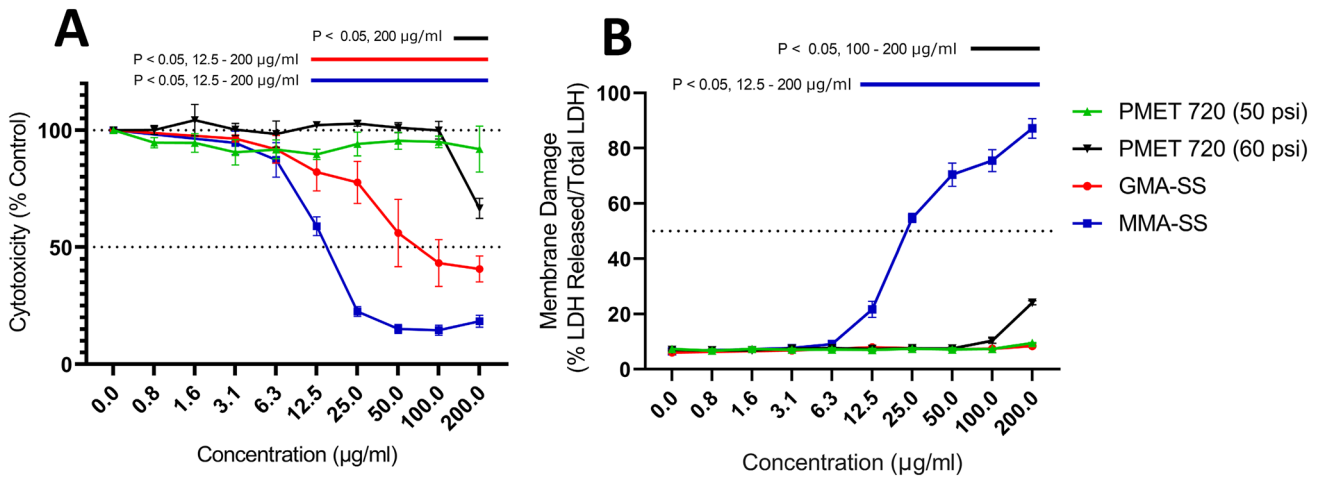

Fig. 6 **A** Cytotoxicity measured by evaluating the change in WST-1 metabolism in macrophages exposed to 0 to 200 µg/ml of either GMA-SS, MMA-SS, PMET720 (50 psi) or (60 psi) particle samples. **B** Dose–response relationship in membrane damage induced by exposure to GMA-SS, MMA-SS, PMET720 (50 psi) or (60 psi) particle samples. The bars above the charts represent significant responses ($p < 0.05$) from control, unexposed cells

PMET720 (60 psi) induced a significant change only at the two highest tested concentrations of 100 and 200 µg/ml (Fig. 6B). GMA-SS particle exposure altered WST-1 metabolism but did not cause membrane damage in the dose range tested. MMA-SS treatment induced a dose-dependent increase in membrane damage and a statistically significant change from 12.5 µg/ml. The EC 50 for PMET720 (50 psi), (60 psi) and GMA-SS was > 200 µg/ml (i.e., the highest dose tested). The EC 50 for MMA-SS was 21 µg/ml ($R^2 = 0.99$, 95% CI 18.6–23.9 µg/ml).

Acellular and in vitro screening for oxidative stress

The acellular oxidative stress potential of PMET720 (50) and (60) psi thermal spray coating particles was assessed by their ability to produce Fenton-like short-lived free radical intermediates in a cell-free system using EPR in the presence of a spin trap (DMPO, 5,5-dimethyl-1-pyrroline N-oxide) and an oxidant (H_2O_2). Chromium (VI) was used as positive control and had the highest change in the EPR peak (Fig. 7A, B). The two PMET720 samples did produce the typical 1:2:2:1 spectrum, which is characteristic for OH. However, the average signal intensity was significantly less than what was observed for the two well-characterized stainless steel particle samples and the Cr (VI) positive control. Although small, the PMET720 (60 psi) sample produced significantly more radicals compared to the PMET720 (50 PSI) sample. The rank order in which the particulate produced free radicals was MMA-SS > GMA-SS > PMET720 (60 psi) > PMET720 (50 PSI). The amount of intracellular reactive oxygen species (ROS) generated in the macrophages was assessed after 24 h of exposure to 0, 6.25, 25

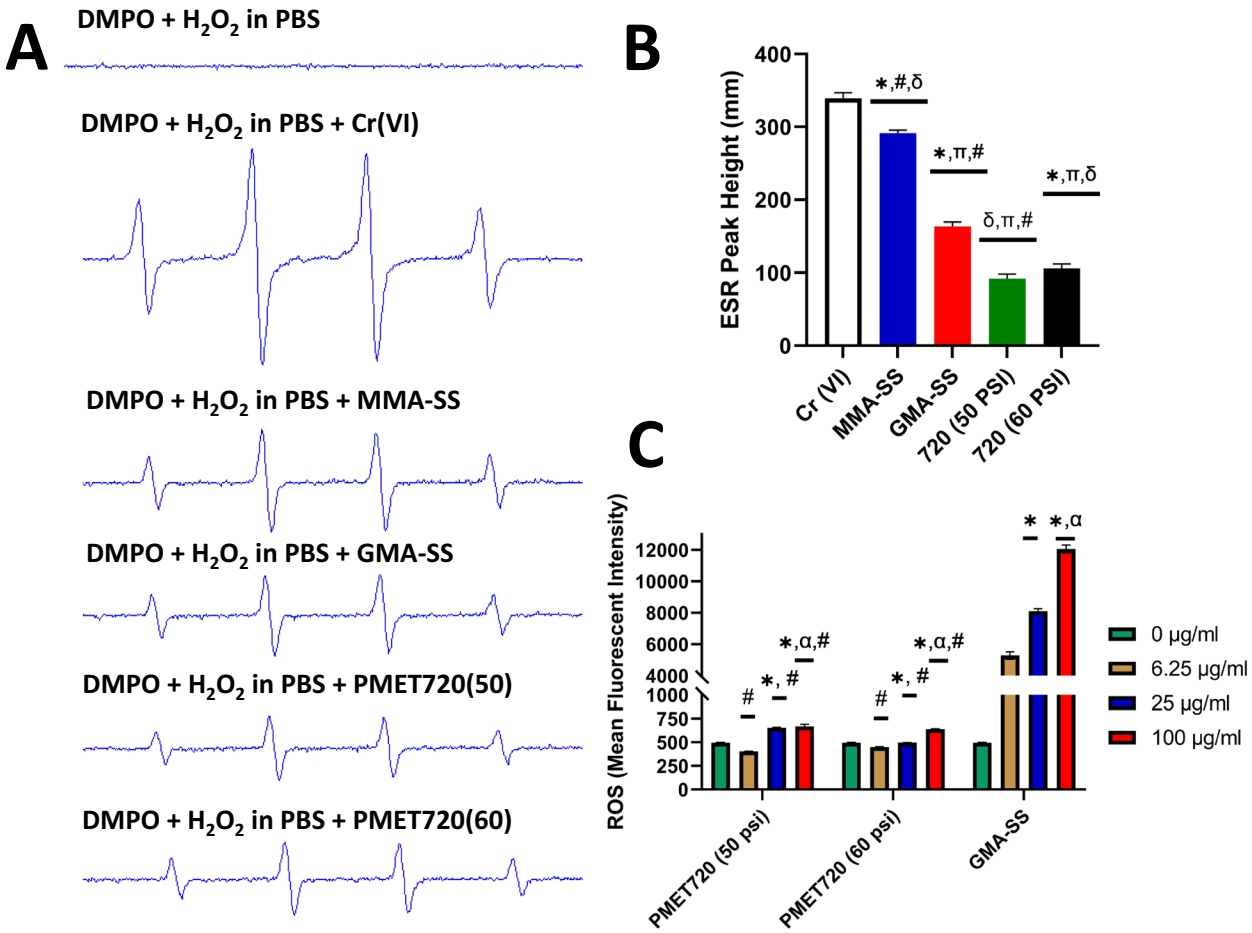

Fig. 7 **A** EPR spectra and **B** EPR peak height with negative control, positive control [(2 mM Cr (VI)], MMA-SS and GMA-SS welding fumes, thermal spray coating samples generated with PMET720 50 psi and 60 psi. Data analyzed by one way ANOVA. *, $^{\#}$, $^{\delta}$ and $^{\pi}$ denote $p < 0.05$ *vs*. PMET 720 (50 psi), PMET 720 (60 psi), GMA-SS and MMA-SS, respectively. **C** Intracellular ROS produced after exposure to 0–100 µg/ml thermal spray coating particulate PMET720 (50 psi and 60psi) and welding fume particulate, GMA-SS. Statistical significance was determined by modeling across dose and treatment group by two-way ANOVA, * and $^{\alpha}$ denote $p < 0.05$ from 0 and 6.25 µg/ml treatments within the group. $^{\#}$Denotes significance from GMA-SS exposure at equivalent dose

and 100 µg/ml of PMET720 (50 psi), PMET720 (60 psi), or GMA-SS (Fig. 7C). There was no difference in the level of intracellular ROS generated due to exposure of PMET720 (50 psi) and PMET720 (60 psi). GMA-SS caused a significant change from PMET720 (50 psi) and PMET720 (60 psi) at all the doses evaluated. Compared to control cells with no exposure, all the tested particle samples caused a significant change in intracellular ROS generated from 25 µg/ml.

Screening for NF-κB/AP-1 activity in vitro

The signaling transduction pathway NF-kB/AP-1 has been shown to play a critical role in the induction of toxicity due to exposure of welding fumes (Hałatek et al. 2018; McNeilly et al. 2005). NF-kB/AP-1 activity due to exposure of the novel PMET720 (50 psi) and (60 psi) thermal spray coating particles was assessed using the macrophage NF-kB/AP-1 reporter cell line (RAW-Blue™ cell line). These cells secrete embryonic alkaline phosphatase (SEAP) when NF-κB/ AP-1 signaling pathway gets activated due to exposure of the particulate. A dose-dependent increase in NF-kB/AP-1 activity was observed with all the four particle groups compared to unexposed control cells (Fig. 8A). The highest dose evaluated (12.5 µg/ml) induced a 10-, 7-, 3- and two fold increase in NF-kB/AP-1 activity with the MMA-SS, GMA-SS, PMET720 (60 psi) and (50 psi) particle samples, respectively. The lowest dose evaluated (1.56 µg/ml) first showed significant induction in NF-kB/AP-1 activity with both the MMA-SS welding fume and the PMET720 (60 psi) thermal spray coating sample. GMA-SS and PMET720 (50 psi) particle samples showed statistical significance at and above 3.12 µg/ml.

Mechanism of uptake

Assessing the uptake after inhibiting various internalization pathways revealed that within the 3 h of exposure, PMET720 thermal spray particles were internalized using both endocytic and phagocytic/pinocytic mechanisms. The change in uptake observed with clathrin-, caveolin-, and actin-dependent pinocytosis/phagocytosis was 54%, 76% and 63%, respectively (Fig. 8B). While the particulate was internalized by various mechanisms, particle uptake through clathrin-mediated endocytosis appears to be the major mechanism of uptake. The heterogeneity in internalization may be due to the wide size distribution of the PMET720 thermal spray coating sample (Fig. 2).

Discussion

Thermal spray coating processes generate high emissions of metal rich ultrafine particulates. These emissions have been reported to be far higher than particulates generated

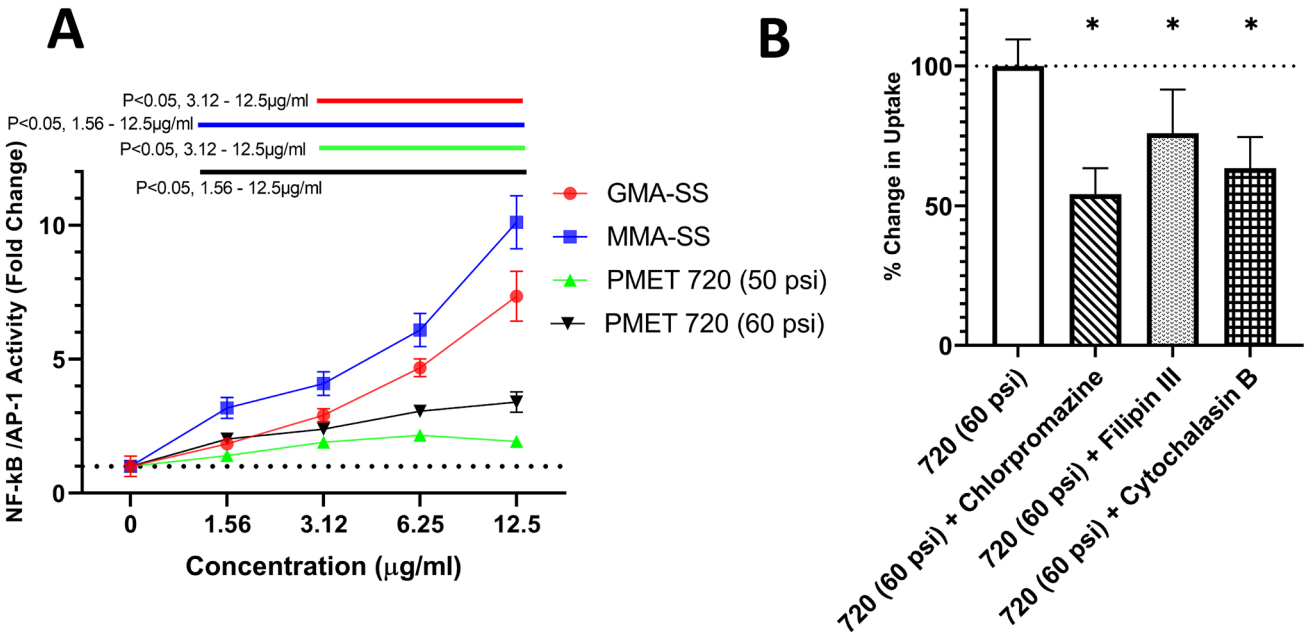

Fig. 8 **A** NF-kB/AP-1 activation after exposure to 0–12.5 µg/ml GMA-SS, MMA-SS, PMET720 (50 psi) and (60 psi) particle samples. The colored bars above highlight statistical significance ($p < 0.05$) from unexposed control cells. **B** Mechanism of uptake of PMET720 (60 psi) thermal spray coating particles and GMA-SS welding particle samples. *Significant ($p < 0.05$) change in uptake from control cells without inhibitor treatment

(concentrations > 10^8 particles/cm^3) using other metal processing procedures, like electric arc welding (Bemer et al. 2010). Despite efforts to provide adequate ventilation, occupational exposure limits have been observed to be exceeded in multiple evaluations, such as 34.2 mg/m^3 for the total dust in China (Huang et al. 2016) and 12.4–22.5 mg/m^3 for total suspended particle concentration in Greece (Petsas et al. 2007). Like welding fumes, aerosols from thermal spray coating processes contain comparable metal constituents, some of which are carcinogenic (e.g., Cr). Because of this, welding fumes have been classified by the World Health Organization's International Agency for Research on Cancer (IARC) as Group 1 carcinogen (IARC 2018).

Hexavalent Cr exposures have been measured in different facilities performing thermal spray coating by different industrial hygiene groups to be as high as 100 times the OSHA permissible exposure limit of 5 µg/m^3 and 20–40 times higher than the permissible exposure limit for a 12-h work shift (Antonini et al., 2021). Also, Cr levels were measured to be 15 times higher than the occupational exposure limit after spray coating metal materials containing Cr and Cr oxides at worksites in France (Darut et al. 2021b). Because thermal spray coating is an emerging industry and adverse health effects from thermal spray coating have not been thoroughly investigated, there is a need to evaluate the potential of pulmonary toxicity caused by exposure of these spray coating aerosols.

In the current work, the aerosols generated by thermal spray coating were studied using a recently developed, automated thermal spray coating generator (Afshari et al., 2022) with a consumable stainless steel PMET720 wire, the most commonly used wire in U.S. industries. The metal-rich aerosol was composed of Fe (82%), Cr (13%), Mn (2%), and Zn (1%) and had a MMAD of approximately 0.30 µm. SEM images of the collected spray coating aerosols showed chain-like aggregates of ultrafine primary particles, similar to what was observed by others for thermal spray coating particles (Bemer et al. 2010). Based on the similarity of the processes and composition of the consumable metal wires used, it is not unexpected that the particles formed during stainless steel thermal spray coating were not that different in terms of metal profile as well as particle size and morphology to stainless steel particles generated during welding. There were differences observed when comparing the metal amounts measured in thermal spray coating samples (Fe: 81.7–82.2%; Cr: 13.4–14.9%; Mn: 2.37–2.61%; Ni 0.26–0.40%) *versus* the welding fume samples (Fe: 42.0–57.2%; Cr: 20.3–28.1%; 13.8–16.2%; Ni: 2.84–8.51%) used in the current study. These differences were due to different metal profiles of the consumable wires used in either the welding or thermal spray coating processes as the composition of the generated particles have been shown to come primarily from the consumption of the metal wire (Antonini 2003). Importantly, the most toxic metals (e.g., Cr, Ni, Mn) were elevated in the welding fume samples compared to the thermal spray coating samples.

Using the inhalation exposure system rats were exposed by inhalation to 25 mg/m^3 of PMET720 (60 psi) thermal spray coating aerosol for 4 h a day for 9 consecutive days. Pulmonary injury, inflammation, and alteration in cytokine and chemokines in the lung were evaluated. Resolution and kinetics of the lung injury and inflammation were assessed at 1, 7, 14, and 28 d after the last day of exposure. The level of LDH in BAL fluid, a marker of lung damage, and lung inflammation, as assessed by BAL cellularity, was significantly increased compared to air-exposed controls only after 1 day after exposure, with the animals recovering by day 7 after exposure. The kinetics of this response to the thermal spray coating aerosol was observed to be quite different compared to stainless steel welding fume inhalation exposure.

Animals that were exposed to GMA-SS welding fume (40 mg/m^3) for 3 day did not show elevations in lung inflammation until after 6 day after the last exposure (Antonini et al. 2007). It was previously observed that the GMA-SS particles inhibited chemotactic signaling in the lung as well as altering the function of alveolar macrophages. Exposure to the GMA-SS welding fume delayed the overproduction of the chemokine, MIP-2, and had no effect on production of the inflammatory cytokine, TNF-α. A significant elevation in MIP-2 was not observed until 4 day after exposure. This elevation in MIP-2 immediately preceded the increase in lung PMN influx. In addition, alveolar macrophage function, as measured by chemiluminescence, was suppressed early after welding fume exposure.

Unlike the previous stainless steel welding fume study, animals exposed to PMET720 thermal spray coating aerosols in the current study developed a significant up-regulation in seven chemokines or cytokines (IL-18, MIP-1α, VEGF, LIX, fractalkine, IP-10, and EGF) in BAL fluid at 1 day after exposure. By 7 day, only MIP-1α and fractalkine were significantly different, both being down-regulated, from air controls after thermal spray coating aerosol exposure. This cytokine response after thermal spray coating exposure was in line with the quick resolution of the lung injury and inflammatory response that was observed in the animals, despite the persistence of the particles in the macrophages at 28 day after exposure.

In many cases, welding fumes have been observed to persist in the lung macrophages for weeks to months with little to no injury or inflammation present (Antonini et al. 2013, 2011; Hicks et al. 1983).The difference in the lung response of stainless-steel welding fumes compared to what was observed with the thermal spray coating aerosol exposure is likely do to the difference in the amounts of Cr, Ni, and Mn present in the samples. The results of previous welding

fumes studies have indicated that the pulmonary response was primarily dependent on metal composition (Taylor et al. 2003; Erdely et al. 2011; Antonini et al. 2011). It is also important to note that some forms of Fe and Fe-abundant particulate matter exposure may contribute to the lung responses (Zeidler-Erdely et al. 2019), sometimes presenting without toxicity but causing immunosuppression and lung tumor promotion (Falcone et al. 2018; Kodali et al. 2013). To address these challenges, further studies over a longer period are currently ongoing to evaluate more chronic lung responses and the persistence (half-life) of a variety of thermal spray coating particles with different metal profiles.

The intracellular uptake mechanism of particles is dependent on the physicochemical properties of the particulate (i.e., size, shape and charge). The intracellular trafficking, signaling and fate of the particle after exposure are dependent on the mechanism of internalization. The mechanism of uptake of the PMET720 (60 psi) thermal spray coating sample was systematically evaluated using pharmaceutical transport inhibitors. Chlorpromazine and filipin III were used to inhibit clathrin- and caveolin-mediated endocytosis, respectively. Actin cytoskeleton-driven pinocytosis and phagocytosis were inhibited by treating the cells with cytochalasin B. Clathrin-coated pits occupy 0.5–2% of the cell surface and the upper limit for particulates internalized via clathrin-coated vesicles is ~ 100 nm (Rennick et al. 2021). Caveolae are 50–80 nm flask- shaped membrane invaginations that are abundant on the cell surface and play an important role in the uptake of several pathogens and viruses. Particles larger than 200 nm are typically internalized by actin-driven pinocytosis and phagocytosis (Behzadi et al. 2017). For the thermal spray particulate, characterizing the route of uptake using pharmaceutical inhibitors showed all the pathways had a role in the uptake. Inhibition of clathrin-mediated endocytosis caused the most inhibition. The wide size distribution of the particles could be the reason for internalization via a myriad of pathways.

In vitro, exposure to the thermal spray aerosols induced cytotoxicity and membrane damage only at the highest dose tested. The cytotoxicity of PMET 720 coating particulate was low ($IC_{50} > 200$ µg/ml) compared to stainless steel welding fumes GMA-SS ($IC_{50} = 35$ µg/ml) and MMA-SS ($IC_{50} = 13$ µg/ml) used as particulate controls. The welding fumes were chosen as controls as they are metal rich incidental particulate that have similar morphology (chain like aggregates) similar to thermal spray coating particulate. The toxicity profile of the welding fumes is well characterized, and the molecular mechanisms of toxicity induced by these welding fumes has been extensively investigated (Antonini 2003; Antonini 2014; Kodali et al. 2020; Leonard et al. 2010; McCarrick et al. 2019; McNeilly et al. 2005; Shoeb et al. 2017; Zeidler-Erdely et al. 2010). NF-kB/AP-1 pathway activation and regulation of oxidative stress and inflammation have been shown to be the leading mechanisms of toxicity for welding fumes and other metal rich particulate (Graczyk et al. 2016; Kodali and Thrall 2015; Lodovici and Bigagli 2011; McNeilly et al. 2005; Riccelli et al. 2020). The PMET720 thermal spray particulates were screened for these known mechanisms of toxicity and their potency was compared with welding fume particulates. Acellular evaluation of oxidative stress potential by EPR indicated the welding fume spray particulate was reactive and generated free radicals. In line with the acellular findings, in vitro studies indicated that these particulates induced intracellular ROS. The acellular reactivity and intracellular ROS produced was several fold lower than that produced by welding fume particulate. The spray coating particulate activated NF-kB/AP-1 and at the highest dose tested, i.e., 12.5 µg/ml, PMET720 (60 psi), particulate caused 2- to threefold lower activation than GMA-SS and MMA-SS welding fumes. The cytotoxicity and mechanism-based screening also showed that although there were some changes between the PMET720 thermal spray coating aerosols generated at 50 psi and 60 psi, the toxicity profile did not substantially change in relation to the coating pressure. In comparison with the stainless-steel welding fume particulates evaluated, the PMET720 thermal spray coating particulates were less toxic. Thermal spray coatings contained twice as much Fe and half of the more toxic metals like Cr; the altered toxicity observed could be due to the different metal composition and the resulting dissolution. In the current work, we evaluated the toxicity of thermal spray particulate generated using PMET720.

Conclusion

The current work demonstrates that thermal spray coating particulates generated from PMET720 stainless steel wire exhibited acute pulmonary toxicity and inflammation, albeit to a smaller extent compared to welding fumes. The toxicity induced by the PMET720 thermal spray coating particulates, like other metal rich aerosols, induced toxicity by activating NF-kB/AP-1 and oxidative stress pathway. The in vivo lung damage and inflammation was resolved by day 7 after the last day of the inhalation exposure. The particles were retained in the lung even after 28 days after exposure and were internalized via clathrin-mediated endocytosis, caveolae-mediated endocytosis and actin-driven phagocytosis/pinocytosis. Additional studies are needed to determine effects of thermal spray coating aerosols generated using wires composed of other metal compositions, and the biopersistence of the particulate and the potential health hazards resulting from bio- persistence.

Disclaimer

The findings and conclusions in this report are those of the authors and do not necessarily represent the official position of the National Institute for Occupational Safety and Health, Centers for Disease Control and Prevention. Mention of brand name does not constitute product endorsement.

Funding Funding was provided by the National Institute for Occupational Safety and Health project # 93909NE and National Institute of Health funding R01 ES031253.

Data availability The data from this project will be posted in the NIOSH Data and Statistics Gateway https://www.cdc.gov/niosh/data/default.html.

Conflict of interest All the authors declare that they have no competing interests.

References

Afshari AA, McKinney W, Cumpston JL et al (2022) Development of a thermal spray coating aerosol generator and inhalation exposure system. Toxicol Rep 9:126–135. https://doi.org/10.1016/j.toxrep.2022.01.004

Antonini JM (2003) Health effects of welding. Crit Rev Toxicol 33(1):61–103. https://doi.org/10.1080/713611032

Antonini JM (2014) 8.04 - Health effects associated with welding. In: Hashmi S, Batalha GF, Van Tyne CJ, Yilbas B (eds) Comprehensive materials processing. Elsevier, Oxford, pp 49–70

Antonini JM, Stone S, Roberts JR et al (2007) Effect of short-term stainless steel welding fume inhalation exposure on lung inflammation, injury, and defense responses in rats. Toxicol Appl Pharmacol 223(3):234–245. https://doi.org/10.1016/j.taap.2007.06.020

Antonini JM, Roberts JR, Stone S et al (2011) Persistence of deposited metals in the lungs after stainless steel and mild steel welding fume inhalation in rats. Arch Toxicol 85(5):487–498. https://doi.org/10.1007/s00204-010-0601-1

Antonini JM, Roberts JR, Schwegler-Berry D, Mercer RR (2013) Comparative microscopic study of human and rat lungs after overexposure to welding fume. Ann Occup Hyg 57(9):1167–1179. https://doi.org/10.1093/annhyg/met032

Antonini JM, McKinney WG, Lee EG, Afshari AA (2021) Review of the physicochemical properties and associated health effects of aerosols generated during thermal spray coating processes. Toxicol Ind Health 37(1):47–58. https://doi.org/10.1177/0748233720977975

ASM Thermal spray technology white paper prepared by the Thermal Spray Society affiliate of ASM International. In: ASM Thermal Spray Society. http://www.asminternational.org/web/tss/technical/white-paper Accessed 09 2021

Behzadi S, Serpooshan V, Tao W et al (2017) Cellular uptake of nanoparticles: journey inside the cell. Chem Soc Rev 46(14):4218–4244. https://doi.org/10.1039/c6cs00636a

Bemer D, Regnier R, Subra I, Sutter B, Lecler MT, Morele Y (2010) Ultrafine particles emitted by flame and electric arc guns for thermal spraying of metals. Ann Occup Hyg 54(6):607–614. https://doi.org/10.1093/annhyg/meq052

Chadwick J, Wilson H, White M (1997) An investigation of occupational metal exposure in thermal spraying processes. Sci Total Environ 199(1–2):115–124

Darut G, Dieu S, Schnuriger B et al (2021a) State of the art of particle emissions in thermal spraying and other high energy processes based on metal powders. J Clean Prod 303:126952

dos Santos T, Varela J, Lynch I, Salvati A, Dawson KA (2011) Effects of transport inhibitors on the cellular uptake of carboxylated polystyrene nanoparticles in different cell lines. PLoS ONE 6(9):e24438. https://doi.org/10.1371/journal.pone.0024438

Falcone LM, Erdely A, Kodali V et al (2018) Inhalation of iron-abundant gas metal arc welding-mild steel fume promotes lung tumors in mice. Toxicology 409:24–32. https://doi.org/10.1016/j.tox.2018.07.007

Gérard B (2006) Application of thermal spraying in the automobile industry. Surf Coat Technol 201(5):2028–2031. https://doi.org/10.1016/j.surfcoat.2006.04.050

Graczyk H, Lewinski N, Zhao J et al (2016) Increase in oxidative stress levels following welding fume inhalation: a controlled human exposure study. Part Fibre Toxicol 13(1):31. https://doi.org/10.1186/s12989-016-0143-7

GrandViewResearch Thermal spray coatings market size worth $14.1 billion by 2028., vol 2021. Grand View Research

Hałatek T, Stanisławska M, Świercz R, Domeradzka-Gajda K, Kuraś R, Wąsowicz W (2018) Clara cells protein, prolactin and transcription factors of protein NF-κB and c-Jun/AP-1 levels in rats inhaled to stainless steel welding dust and its soluble form. Int J Occup Med Environ Health 31(5):613–632. https://doi.org/10.13075/ijomeh.1896.01234

Hardwicke CU, Lau Y-C (2013) Advances in thermal spray coatings for gas turbines and energy generation: a review. J Therm Spray Technol 22(5):564–576

Herman H, Sampath S, McCune R (2000) Thermal spray: current status and future trends. MRS Bull 25(7):17–25

Hicks R, Al-Shamma KJ, Lam HF, Hewitt PJ (1983) An investigation of fibrogenic and other toxic effects of arc-welding fume particles deposited in the rat lung. J Appl Toxicol 3(6):297–306. https://doi.org/10.1002/jat.2550030605

Huang H, Li H, Li X (2016) Physicochemical characteristics of dust particles in HVOF spraying and occupational hazards: case study in a Chinese company. J Therm Spray Technol 25(5):971–981. https://doi.org/10.1007/s11666-016-0422-8

IARC (2018) Welding, molybdenum trioxide, and indium tin oxide Working Group on the Evaluation of Carcinogenic Risks to Humans. vol 118. World Health Organization, p 36–265

Ibuki Y, Toyooka T (2012) Nanoparticle Uptake Measured by Flow Cytometry. In: Reineke J (ed) Nanotoxicity: Methods and Protocols. Humana Press, Totowa, NJ, pp 157–166

Kodali V, Thrall BD (2015) Oxidative stress and nanomaterial-cellular interactions. In: Roberts SM, Kehrer JP, Klotz L-O (eds) Studies on experimental toxicology and pharmacology. Springer International Publishing, Cham, Oxidative Stress in Applied Basic Research and Clinical Practice, pp 347–367

Kodali V, Littke MH, Tilton SC et al (2013) Dysregulation of macrophage activation profiles by engineered nanoparticles. ACS Nano 7(8):6997–7010. https://doi.org/10.1021/nn402145t

Kodali V, Shoeb M, Meighan TG et al (2020) Bioactivity of circulatory factors after pulmonary exposure to mild or stainless steel welding fumes. Toxicol Sci 177(1):108–120. https://doi.org/10.1093/toxsci/kfaa084

Leonard SS, Xia C, Jiang BH et al (2003) Resveratrol scavenges reactive oxygen species and effects radical-induced cellular responses. Biochem Biophys Res Commun 309(4):1017–1026. https://doi.org/10.1016/j.bbrc.2003.08.105

Leonard SS, Jenny R, James M, Castranova V, Shi X (2004) PbCrO 4 mediates cellular responses via reactive oxygen species. Mol Cell Biochem 255(1):171–179

Leonard SS, Chen BT, Stone SG et al (2010) Comparison of stainless and mild steel welding fumes in generation of reactive oxygen species. Part Fibre Toxicol 7(1):32. https://doi.org/10.1186/1743-8977-7-32

Lodovici M, Bigagli E (2011) Oxidative stress and air pollution exposure. Journal of Toxicology 2011:487074. https://doi.org/10.1155/2011/487074

Malek MHA, Saad NH, Abas SK, Shah NM Thermal arc spray overview. In: IOP Conference Series Materials Science and Engineering (Online), 2013. vol 46.

McCarrick S, Wei Z, Moelijker N et al (2019) High variability in toxicity of welding fume nanoparticles from stainless steel in lung cells and reporter cell lines: the role of particle reactivity and solubility. Nanotoxicology 13(10):1293–1309. https://doi.org/10.1080/17435390.2019.1650972

McNeilly J, Jimenez LA, Clay MF et al (2005) Soluble transition metals in welding fumes cause inflammation via activation of NF-kappaB and AP-1. Toxicol Lett 158(2):152–157. https://doi.org/10.1016/j.toxlet.2005.03.005

BLS Occupational employment and wages (2020) 51–924 Coating, painting, and spraying machine setters, operators, and tenders. In: U.S. Bureau of Labor Statistics. https://data.bls.gov/cgi-bin/print.pl/oes/current/oes519121.htm Accessed 08 2021

Oerlikon An introduction to thermal spray. In: Oerlikon Metco. https://www.oerlikon.com/ecomaXL/files/metco/oerlikon_BRO-0005.6_Thermal_Spray_Brochure_EN.pdf Accessed 09 2021

Petsas N, Kouzilos G, Papapanos G, Vardavoulias M, Moutsatsou A (2007) Worker exposure monitoring of suspended particles in a thermal spray industry. J Therm Spray Technol 16(2):214–219. https://doi.org/10.1007/s11666-007-9027-6

Plummer EM, Manchester M (2013) Endocytic uptake pathways utilized by CPMV nanoparticles. Mol Pharm 10(1):26–32. https://doi.org/10.1021/mp300238w

Rennick JJ, Johnston APR, Parton RG (2021) Key principles and methods for studying the endocytosis of biological and nanoparticle therapeutics. Nat Nanotechnol 16(3):266–276. https://doi.org/10.1038/s41565-021-00858-8

Riccelli MG, Goldoni M, Poli D, Mozzoni P, Cavallo D, Corradi M (2020) Welding fumes, a risk factor for lung diseases. Int J Environ Res Public Health 17(7):2552. https://doi.org/10.3390/ijerph17072552

Shoeb M, Kodali V, Farris B et al (2017) Evaluation of the molecular mechanisms associated with cytotoxicity and inflammation after pulmonary exposure to different metal-rich welding particles. Nanotoxicology 11(6):725–736. https://doi.org/10.1080/17435390.2017.1349200

Stefaniak AB, Harvey CJ, Bukowski VC, Leonard SS (2009) Comparison of free radical generation by pre-and post-sintered cemented carbide particles. J Occup Environ Hyg 7(1):23–34

Suzuki H, Toyooka T, Ibuki Y (2007) Simple and easy method to evaluate uptake potential of nanoparticles in mammalian cells using a flow cytometric light scatter analysis. Environ Sci Technol 41(8):3018–3024. https://doi.org/10.1021/es0625632

Vranic S, Boggetto N, Contremoulins V et al (2013) Deciphering the mechanisms of cellular uptake of engineered nanoparticles by accurate evaluation of internalization using imaging flow cytometry. Part Fibre Toxicol 10(1):2. https://doi.org/10.1186/1743-8977-10-2

Zeidler-Erdely PC, Kashon ML, Li S, Antonini JM (2010) Response of the mouse lung transcriptome to welding fume: effects of stainless and mild steel fumes on lung gene expression in A/J and C57BL/6J mice. Respir Res 11(1):1–18. https://doi.org/10.1186/1465-9921-11-70

Zeidler-Erdely PC, Falcone LM, Antonini JM (2019) Influence of welding fume metal composition on lung toxicity and tumor formation in experimental animal models. J Occup Environ Hyg 16(6):372–377. https://doi.org/10.1080/15459624.2019.1587172

Zucker RM, Massaro EJ, Sanders KM, Degn LL, Boyes WK (2010) Detection of TiO_2 nanoparticles in cells by flow cytometry. Cytometry A 77(7):677–685. https://doi.org/10.1002/cyto.a.20927